Identifiers: NCT03230981 Unique Protocol ID: 2017P000867

Brief Title: Age-dependency of Cornea Biomechanics Using OCT Vibrography

I. BACKGROUND AND SIGNIFICANCE

A) Background

The cornea, the clear front window of the eye, consists of finely intertwined collagen fibers, which give the cornea a microstructure that provides mechanical integrity necessary to maintain its typical dome-shape against the intraocular pressure (IOP). Changes in the biomechanical properties can lead to an abnormal corneal shape and refractive errors. As a result, light is not perfectly focused onto the retina and the vision is affected. A typical example of alterations in the cornea's biomechanical properties is found in patients with an eye disorder called Keratoconus, which leads to progressive thinning of the cornea. Keratoconus explants have shown disrupted collagen orientation [1] and decreased mechanical modulus [2]. Similar findings have been observed in corneas that developed ectasia after refractive surgery like LASIK (laser-assisted in situ keratomileusis, the most widely performed type of refractive surgery), where a laser is used to reshape the cornea [3]. With LASIK surgery becoming increasingly popular (more than 28 million LASIK procedures have been performed worldwide), the incidence of post-LASIK ectasia has increased continuously.

Numerous studies have shown that promising interventions like collagen crosslinking (CXL) can slow down an arrest progression of ectatic eye diseases [4]. Keratoconus, as a typical example, although it cannot be cured, could be at least halted by CXL. Therefore, early diagnosis of ectasia is crucial for the patient. Current diagnostic methods of ectasia are based on morphological rather than biomechanical analysis. The irregular patterns of the cornea can be detected by pachymetry and topography before clinical signs occur, but these tests cannot reliably differentiate truly weak or keratoconic corneas from atypical normal ones [5, 6].

Additionally, the screening protocols for LASIK surgery that rely on indirect morphological risk factors have had limited success in the clinic. About 15% of patients seeking laser vision correction are considered at-risk and are thus denied treatment. On the other hand, patients with normal appearing pachymetry and topography and no other risk factors have gone on to develop post-LASIK ectasia [7-9].

These are compelling needs for improved diagnostic methods. More recently, and triggered by those unmet needs, an interest in the mechanical properties of the cornea has emerged. Typical examples of mechanical properties are elastic modulus and corneal stiffness. The corneal stiffness is known to increase with age with the behavior closely fitting an exponential power function typical of collagenous tissue [10]. Further research suggests that corneal stiffness increases by as much as a factor of approx. 2 between the ages of 20 and 100 years [11].

The connection of the mechanical properties to the pathophysiology of the condition of the cornea makes them highly suited for early identification of patients at risk to develop ectasia [9, 12]. Consequently, there have been considerable efforts to develop noninvasive, sensitive methods to characterize corneal biomechanics in vivo. The most widely used approach employs air-puffs to induce a burst of pressure on the cornea and analyzes corneal deformation and recovery. The Ocular Response Analyser, for example, is an instrument based on this principle and has been approved for in vivo measurement of properties, so-called corneal hysteresis, which is associated with viscous damping of tissue deformation [13]. Corneal hysteresis has shown to be reduced in ectatic disease, but its sensitivity and specificity have been insufficient to differentiate normal eyes from low-grade keratoconus [14]. Air-puff can be combined with Scheimpflug camera [15] or optical coherence tomography (OCT) [16] for image-based analysis and estimates of corneal viscoelastic parameters [17]. Other emerging techniques for measuring elastic modulus with spatial resolution include supersonic shear imaging [18], optical coherence elastography [19-24], and Brillouin microscopy [25].

In this pilot study we propose to investigate the ability of OCT Vibrography to determine cornea material parameters. More precisely, we want to study the oscillation response in human corneas in vivo using sound excitation (110-110dB) together with phase-sensitive OCT to measure the frequency response function of the human cornea in vivo and to analyze the dependency of the frequency response function on age. Additionally we will use Brillouin Microscopy data for computer simulations to validate OCT Vibrography results.

The level of light exposure to the retina, cornea, and skin are within the safety standards as described by the ANSI Z136.1-2014 safety standard. A detailed laser safety calculation is added in Section XII.

B) Swept-Source Optical Coherence Tomography (OCT)

Over the past two decades, OCT has undergone a rapid development from its technological inception to adoption as standard-of-care in ophthalmology. Swept-Source OCT (or, Optical Frequency Domain Imaging, OFDI), is a relatively new method for OCT that employs a wavelength-swept light source to probe the amplitude and phase of back scattering light from tissue [26-28]. This frequency-domain method has enabled significant improvements in imaging speed, sensitivity, and ranging depth over conventional time-domain OCT systems, and has been demonstrated for imaging anterior eye segments [28-35]. Compared to Spectral domain OCT, swept source OCT offers several advantages such as immunity to motion-induced signal fading [36], simple polarization-sensitive or diversity scheme [29], and long ranging depth [28]. Swept source OCT has been successfully used to image the human eye in vivo [37].

C) OCT Vibrography

Our group has recently developed a new technique capable of visualizing acoustic vibrations. This technique, named OCT Vibrography, is based on the synchronized acquisition of phase information that is directly related to the vibration of the sample. It was shown that, after post processing of the data, 3-D snapshots of an object vibrating at acoustic frequencies in response to applied stimuli could be obtained [38]. As a proof-of-concept experiment, OCT Vibrography was successfully applied to the visualization of the acoustic resonance modes of a miniature drum driven acoustically at several kHz. Figure 1 (taken from [38]) shows (a) the schematic setup with a latex drum, (b) vibrography snapshot images of a vibrating miniature drum at a frequency of 800 Hz, and (c) a cutaway image showing the motion in a cross-section of the membrane.

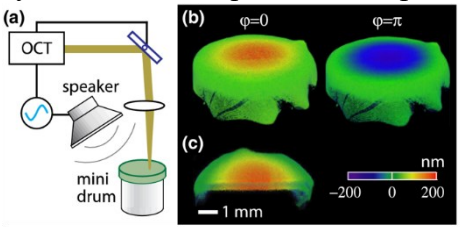

Fig. 1 (a) Schematic setup of OCT Vibrography with a miniature drum and (b-c) OCT Vibrography snapshot images.

D) OCT Vibrography imaging to estimate corneal biomechanics

We have recently demonstrated the ability of OCT Vibrography to observe sound-induced resonance modes of the cornea, and, therewith, to determine corneal biomechanical properties. Experiments were conducted on ex vivo bovine [39, 40] and porcine globes [40], and modal analysis was performed in a finite-element model to study oscillation response and to analyze the dependency of the frequency response function on biomechanical properties and corneal topography, among others.

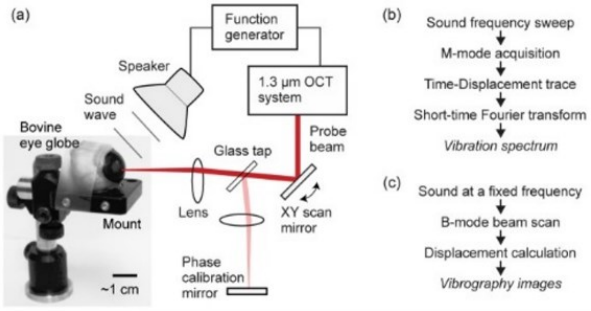

Fig. 2 (a) Schematic of the experimental set up with ex vivo eye globe and (b-c) Signal processing sequences (see text).

The experimental set up consisted of a home-built phase-sensitive OCT system (an updated version of before mentioned device from Chang et al. [38]) which employed a polygon scanner swept laser in the spectral range from 1.23 to 1.34 µm with a typical sweep rate of 45 kHz and an optical power of 15 mW on the sample. The sound source was a high-fidelity loudspeaker, which was controlled by an arbitrary waveform function generator. Figure 2 (taken from [39]) shows the schematic of the set up: The sound wave emitted from the loudspeaker is directed toward the eyeball, and the motion of the cornea is captured and recorded by the OCT system. Figure 2 b) and 2 c) describe the signal processing sequence for the measurement of vibration spectrum at a fixed spatial location in the cornea (b) and to generate vibrography images at a specific sound frequency (c). Figure 3 shows the frequency response curve of a sample measured at the center of the cornea. These results indicated three distinctive peaks at 86 Hz, 200 Hz, and 310 Hz (Figure 3 a). The amplitude of the first peak was around 8µm at 100 dB SPL (2 Pa). The vibration amplitude was proportional to the sound pressure over a range of 80 to 120 dB SPL. The variation in repeated frequency sweeps was less than +/-2%.

Amplitude and frequencies of the modes and their specific spatial distributions in the cornea are thought to provide rich information about the corneas' biomechanics. Further research, especially in vivo, is necessary to understand how different corneal parameters manifest themselves in vibrational resonance, and how these resonances are dependent on age.

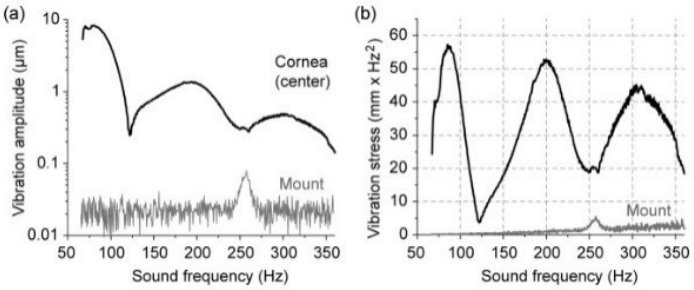

Another relevant biomechanical marker is the velocity of shear acoustic waves in the corneal tissue. There is a direct mathematical relationship between the shear wave velocity and the elastic moduli of the cornea:

$$\mu = \rho c_s^2 \approx \frac{E}{3}$$

where μ is the shear modulus, E is Young's modulus, ρ is the density and c_s is the shear wave velocity. This approach is therefore promising to obtain local and quantitative measurements of corneal biomechanical properties. Figure 4 below shows a typical experiment conducted on ex vivo porcine corneas.

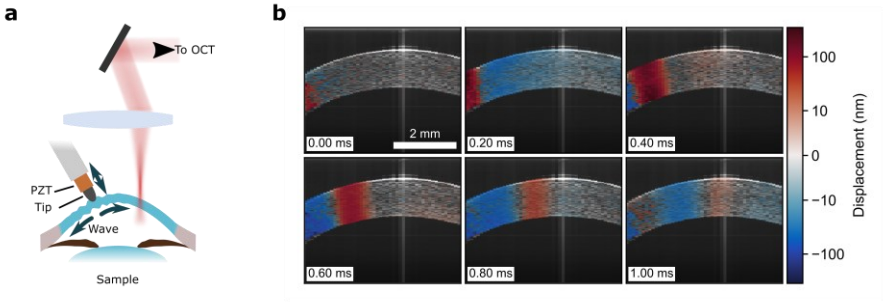

Figure 4. a) Schematic of shear wave generation in the cornea used in previous ex vivo studies. b) Shear wave propagation in the cornea measured by OCT vibrography.

E) Additional Technologies used for Imaging

Brillouin microscopy measurements are planned to support and complement OCT Vibrography data, more specifically, to obtain data of the Brillouin modulus/stiffness. Brillouin Microscopy has recently been developed in our group and has been used in vivo in previously approved Partners IRB protocols: 2015P002404, 2012P002178, 2008P002176. The technique is based on light scattering: When laser light is illuminated to a sample (e.g. the cornea), a portion of the light is reflected due to the acoustic waves that are weak but naturally present in the material by thermal fluctuations [41]. The acoustic waves propagate with a speed that is directly related to the sample's elastic modulus. The acoustic speed (therefore the elastic modulus) is obtained by measuring the frequency shift of the reflected light using a specially designed spectrometer. Combining the spectrometer with a confocal microscope, 3D elasticity imaging can be performed.

The Brillouin data will serve as input data for computer simulations on the cornea's modulus value. Simulations are thought to complement experimental data.

II. SPECIFIC AIMS

In this study we aim to:

- Assess measurement repeatability and overall sensitivity of OCT Vibrography for measurements *in vivo*
- Use OCT Vibrography to measure the mechanical resonance modes of the cornea and their according vibration amplitude in healthy individuals of different ages to investigate age-related changes.
- Use OCT Vibrography to measure the shear wave velocity of the cornea in healthy individuals of different age.
- Use Brillouin Microscopy data for computer simulations to validate OCT Vibrography results

III. SCHEMATIC OF DEVICE

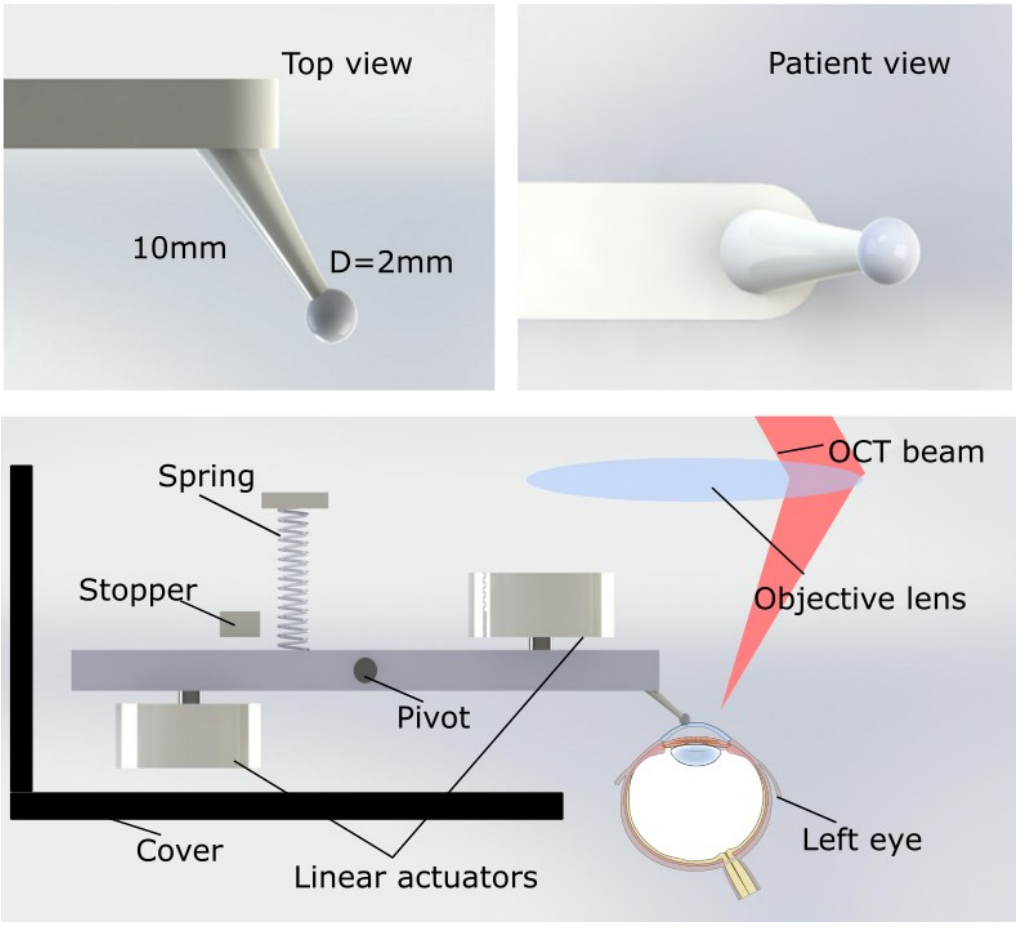

IV. SUBJECT SELECTION

Source of subjects and recruitment methods

Subjects will be recruited as described in the following:

Subject recruitment among MEEI patients

Normal and healthy volunteers (Group 1) and keratoconus patients (Group 2) will be recruited from patients of the contact lens service center at MEEI. The treating ophthalmologist at MEEI will initially introduce the study to the patient, and obtain a patient's permission to be contacted by study staff either (1) verbally during the course of providing medical care or (2) through the use of a recruitment letter.

If the patient agrees, the treating ophthalmologist at MEEI gives approval for their patient to be contacted for research purpose and obtains the patient's permission to be contacted by study staff.

In case a recruitment letter is used for initial contact of the patient, it will be mailed to the potential subjects at least a week prior to the potential subject's eye exam appointment. The subject will be encouraged to contact the research staff or their treating ophthalmologist by phone or email if they have any questions. If the treating ophthalmologist does not hear from the potential subject, they may follow up by phone.

Subject recruitment via email announcements or ad at PHC and MEEI

Normal and healthy volunteers can be recruited by PHC email announcement, the PHC Research website, the MEEI website, or through paper advertisements. Requirement for participation is either (a) having undergone a routine eye exam at MEEI within the last 12 months or (b) having a routine eye exam scheduled and completed at MEEI prior to study enrollment. Potential subjects who are interested in the study will contact the study staff. Eligibility will be determined and a study visit will be scheduled The subject may be contacted by regular mail, electronic mail, or phone call to confirm date and time of scheduled study procedure as well as additional logistical information.

INCLUSION/EXCLUSION CRITERIA

Inclusion criteria

- Male or female subjects between the ages of 18 to 79 years
- Group 1 (N = 80): Healthy normal subjects with no significant eye disease and no significant refractive errors
- Group 2 (N = 10): Patients diagnosed with keratoconus

Exclusion criteria

- Volunteers with implanted intraocular lenses
- Volunteers with LASIK or any other eye surgery, and monocular volunteers
- Volunteers with restricted mobility, who cannot stand up, walk or sit still on a chair without a back
- Subjects who do not or cannot understand the instructions for imaging
- Subjects with diabetes, glaucoma family history
- Subjects who are pregnant and/or breastfeeding.

V. EQUITABLE SELECTION OF SUBJECTS

Subjects will be recruited from the Massachusetts Eye and Ear Infirmary (MEEI) and PHC. Eligibility will be determined by the inclusion/exclusion criteria. There will be no exclusion based on gender or ethnicity.

Because there is no direct benefit to the study, the study only involves the use of a non-marketed device, and we will image healthy subjects, we will not enroll non-English speaking subjects.

VI. SUBJECT ENROLLMENT

Study staff will confirm with potential subjects that they are interested in participating in the research study prior to enrollment in the study. The potential subject will be informed that participation is entirely voluntary and that his/her participation will not affect his/her healthcare now or in the future. If the potential subject is willing to participate in the research study, consent will be obtained by trained study staff. During the visit, the study procedures will be explained and any questions will be answered. Because all imaging devices used in this study are non-significant risk devices, and the study procedures will not interfere in any way with the standard of care procedures or medical care that the subjects would otherwise receive, approved study staff members can obtain the signed informed consent from the subject. Obtaining informed consent does not need to be limited to licensed physicians in this study. The subject will sign the written consent form prior to any scheduled standard of care eye and pupil dilation to avoid difficulties in reading and writing. The time of consent will be added to the signature, together with the date, to document that the informed consent was obtained prior to the imaging session at the Wellman Center. The estimated time for the review and the explanation of the consent form is up to 30 minutes.

Two copies of the signed and dated written consent form will be obtained. The original form will be retained in the research records and securely stored in a locked cabinet. A copy of the signed consent form will be given to the subject.

If a clinical eye exam is performed immediately preceding the study procedures, and in the unlikely scenario that the eye examination reveals a condition that changes the eligibility of the subject, the study staff will inform the subject of this change and further imaging at the Wellman Center will not be performed.

VII. STUDY PROCEDURE

A single visit at the Wellman Center will be scheduled for immediately after the subject's scheduled eye exam. Prior to all imaging sessions, the subject will be given time to ask questions regarding the study. The subject may change his/her mind regarding study participation at any time. The complete session is planned as follows:

-Informed Consent Process: ~30 min

-OCT Vibrography with Brillouin Microscopy Imaging: ~60 min

If eye exam at MEEI immediately precedes study procedures:

-Walk from MEEI to the Wellman Center, MGH: ~ 10-15 min

During the ophthalmology exam, the study doctor may do corneal topography with Pentacam (to map the curvature and thickness of the cornea).

Subjects in Group 1 will be asked if interested in a follow-up visit in future by contacting by phone or email.

Imaging Sessions

The entire session includes OCT Vibrography measurements and Brillouin microscopy measurements. The complete session may take up to 60 minutes. OCT Vibrography and Brillouin imaging may be performed on one or two eyes in a subject depending on eligibility.

<u>Imaging Session 1: OCT Vibrography</u>

Prior to OCT Vibrography measurements, the subject will be administered anesthetic drops (Proparacaine Ophthalmic 0.5%, one drop) by a trained technician. During the imaging session of the cornea, the subject will be seated in a chair with his/her chin and forehead on a chin and forehead rest, respectively. The contact areas will be disinfected with alcohol wipes between volunteers. Both eyes may be sequentially imaged. During scanning, the non-imaged eye will be covered using an eye patch. At operator's instructions, the subject will fix his/her eye on a fixation target. No mechanical devices for immobilizing the eye will be used. The operator will adjust the chin rest and the head position in order to create the best accessible angle to start imaging of the cornea. The operator adjusts the position of the vibrating probe tip until it touches patient's cornea. At this point, the subject sits still for up to 5 seconds while the instrument gathers data. The subject will be asked to comply with the procedure up to 20 times per eye. This repetition of measurement may be necessary since the instrument is highly motion sensitive. If data acquisition after 20

repetitions is not successful, it is probably due to high movement of the subject. In this case, the subject should be dropped from the study.

Each scan may take no longer than 20 seconds, and will be followed by short break. The subject may ask for breaks or stopping the imaging at any point.

Imaging session may be taken on the skin of the healthy subjects as a comparison. Each scan may take no longer than 10 seconds, and no more than 20 scans will be taken.

Imaging Session 2: Brillouin Microscopy

During the imaging session of the cornea the subject will seated in a chair with his/her chin and forehead on a chin and forehead rest, respectively. The contact areas will be disinfected with alcohol wipes between volunteers. During scanning, the non-imaged eye will be covered using an eye patch. At operator's instructions, the subject will fix his/her eye on a fixation target. No mechanical devices for direct immobilization of the eye will be used. The operator will adjust the chin rest, the head position, and the orientation of the Brillouin instrument in order to create the best accessible angle to start imaging of the cornea. The localization of the near infrared light in the eye, and the eye gaze angle will be recorded with a near infrared bright field microscopy. Then, the subject will be asked to hold still while fixing the study eye on the target light or projected object for up to 10s for each data point during which the instrument gathers the Brillouin spectrum. The subject will be asked to comply with this procedure at least six times and up to 30 times per session (depending on subject commitment and time). A break between the imaging scans will be provided to rest and to blink the eye. The subject may ask for breaks or stopping the imaging session at any point. During the pause between imaging sessions, the subject will be asked whether they have felt any discomfort related to their positioning, with the imaging near infrared light (=780nm), or with the imaging procedure.

Renumeration

A remuneration of $50 will be offered for the completion of each imaging session. The volunteers will not be charged for the imaging session at the Wellman Center. There will be no compensation if the subjects are measured on the skin only.

A study subject may contact study PIs for any concerns or questions he/she may have after the study procedures are completed. The contact person at the Wellman Center (MGH) is Andy (SH) Yun, PhD, Phone # 617-768-8698, and the contact person at the MEEI is Amy Watts, MD, Phone # 617-573-3185. There is no extra cost associated with the research study

VIII. STATISTICAL METHODS AND POWER ANALYSIS

Hypothesis: OCT Vibrography is able to detect sound induced resonance modes in the cornea and mode changes with age.

Analysis Plan: The relationship between the age of the subject (continuous explanatory variable) and the change in resonance mode (continuous outcome variable) will be investigated with linear regression.

Sample Size and Power for Group 1: Age-variation in sound induced resonance modes of the cornea has not been previously measured *in vivo.* As an approximation we considered the cornea to be a plate with a Young's Modulus of previously published data of corneas of human corneas with different ages [43]. Furthermore, we used previously published literature which deal with vibrations of circular plates in air [44] and water [45] to calculate resonance modes using above mentioned Youngs Modulus. We estimated the slope of variation in the cornea's (first) resonance mode with age to 5.6 Hz/year. If we measure an expected Gaussian distributed sample of healthy volunteers, we will need to measure 42 subjects to be able to reject the null hypothesis that this slope equals zero with probability (power) 0.9. The Type I error probability associated with this test of this null hypothesis is 0.05.

To account for any potential subjects lost in the study, we will have a total target enrollment of up to 80 subjects.

Sample Size and Power for Group 2: Currently, we do not know the effect size (difference in elastic modulus) required for power calculation. We are interested to test the performance of our device in detecting keratoconus over a small group of patients (N = 10).

IX. RISKS AND DISCOMFORTS

Risks and discomforts: OCT Vibrography

OCT is currently the standard-of-care for ophthalmology procedures and the device used for OCT Vibrography does not change the safety-related optical parameters relative to clinically deployed OCT imaging instruments. The OCT in use is a home built phase-sensitive OCT system which employs a polygon scanner swept laser in the spectral range from 1.23 to 1.34 um with a typical sweep rate of 45 kHz and an optical power of 15 mW on the sample.

Direct contact with the cornea is routinely performed for intraocular pressure screening measurements by clinically-approved devices, including the Goldmann tonometer, TonoPen and iCare. It is a safe and well tolerated procedure provided the following criteria are met:

- Anesthetic drops are used to numb the cornea (eliminates pain and avoids the corneal blinking reflex). The drops will be applied by a trained ophthalmology technician at the beginning of the OCT Vibrography session.
- The contacting surface is smooth and has no sharp edges.
- The applied force is low

To the best of our knowledge, there are no official safety limitations describing the minimum radius of curvature to contact the cornea. Therefore, we use the parameters of an existing clinical instrument (TonoPen XL (Reichert Technologies), which has a diameter of 1mm as the lower bound for our tip radius of curvature.

The force applied by our instrument has 2 components: a steady-state force to ensure contact with the cornea, and an oscillation to generate shear waves in the cornea. The steady-state force is controlled by a spring with a low stiffness constant (a design similar to the Goldmann applanation tonometer). The spring is adjusted to produce a maximum force of 50mN (5g), measured by a calibrated dynamometer. This force level is very low and can barely be felt. The oscillating force generates vibrations in the cornea with an amplitude on the order of 1μm. This vibration level is significantly lower than that produced by approved clinical instruments (air-puff tonometers), which produce vibrations on the order of 1mm, and is therefore considered largely safe. The actuation force for the vibration is provided by a pair of electrodynamic actuators which operate at low voltage (less than 5V).

Risk of infection from the probe tip, chin and headrest (modified rest from a commercial slitlamp) will be minimized by disinfecting the probe, chin rest and forehead rest with alcohol in between subjects. To ensure compliance with the ANSI standards, the light source power used in the OCT imaging is measured before each imaging session. The values are logged into the experiment book for each imaging session and kept on record. If any adjustments are made to the system during a session, the power will be measured and recorded again before continuing the imaging session.

Risks and discomforts: Brillouin Microscopy

Risks are minimal as the Brillouin Ocular Scanner light source power is within ANSI and ISO standards, and it is also less than that of the current commercially available systems that use similar light sources. The Brillouin Ocular Scanner has been approved by the radiation safety office and biomedical engineering office at Massachusetts General Hospital in previously approved IRB protocols. In case of any emergency, a mechanical shutter will block the near infrared laser beam by the push of an emergency button. Subjects will be constantly monitored and asked about their well-being. Risks of infection are minimal as the BOS obtains images without direct contact to the eye itself. Disinfecting the chin and forehead rests with alcohol wipes in between patients minimizes the risk of infection from subject to subject. Discomfort may occur from eye straining due to the subject restraining the blinking reflex during scanning.

We are not aware of any uncommon risks. To ensure compliance with the ANSI 2007 standards, the light source power used in the Brillouin imaging is measured before each imaging session. The values are logged into the experiment book for each imaging session and kept on record. If any adjustments are made to the system during a session, the power will be measured and recorded again before continuing the imaging session.

There may be risks that unknown at this time.

X. POTENTIAL BENEFITS

There are no direct benefits to the study participants. This study may demonstrate the feasibility of using OCT vibrography technology in ophthalmology, which could potentially benefit patients with keratoconus and other eye diseases in the future.

XI. MONITORING AND QUALITY ASSURANCE

The Principal Investigator will be responsible for overseeing all aspects of the study including: ensuring that the study is conducted according to the IRB-approved protocol, performing monitoring of data and confirming compliance of the study, and protecting the rights, safety, and welfare of the subjects. Should the Principal Investigator at any point feel that the health and well-being of the subject is compromised, the study procedures will be immediately suspended. Therefore, the Principal Investigator will be responsible for determining whether the research should be altered or stopped.

Monitoring of the study data will be made to ensure that all aspects of the current, approved protocol/amendment(s) are followed. A monitoring log will be completed for proper documentation.

Subject data will be collected via case report forms. An enrollment log will be maintained and will contain the subject's personal information and hospital record number. It will be only available to the approved study staff members and will be stored in a secure location. Subjects will be assigned a unique number generated when they enroll in the study. This identification number will be the link to the enrollment log.

The Principal Investigator will ensure the accuracy and completeness of the recorded data. The data will be reviewed regularly by the designated study staff and the Principal Investigator.

Adverse events will be reviewed by the Principal Investigator and will be reported to the Human Research Committee within the required time frame and to all participating investigators according to the Partners Human Research Committee guidelines.

Access to study data will be restricted to the study staff listed on the current and approved protocol/amendments(s). Data will be recorded, generated, and stored electronically on a secure, password-protected server at the Wellman Center, MGH.

XII. LASER EXPOSURE SAFETY CALCULATION

A. Description:

A laser exposure safety calculation is added in this section for the OCT Vibrography. The rationale is to make sure the laser power is below the maximum permissible exposure (MPE) of retina, cornea, and skin.

From the calculation, the effective output of the laser power used in this study ($\leqslant$ 15 mW) complies with the ANSI Z136.1-2014 safety standard.

B. Assumptions:

- We use a swept-source laser with wavelength range of 1200-1400nm. MPE for individual wavelengths is calculated in section F below. Because the laser source has a broad spectrum, the average MPE weighted by the spectrum source is calculated in Section G below.
- Exposure time: >10s (safest case)
- Source type: point source (safest case)

C. MPE for ocular exposure (Table 5c) and skin exposure (Table 7b):

Retina (Table 5c): $5.0\ C_C \times 10^{-3}$ [W/cm2]

Cornea (Table 5c): $0.03\ K_\lambda + 0.07$ [W/cm2]

Skin (Table 7b): $0.2\ C_A$

With (from Table 6a):

$C_A = 5.0$

$C_C = 8 + 10^{0.04(\lambda - 1250)}$

$K_\lambda = 10^{0.01\,(1400-\lambda)}$

D. Limiting apertures (Table 8a and 8b)

Skin: 3.5 [mm] diameter; 9.62e-2 [cm2] area

Retina: 7.0 [mm] diameter; 0.385 [cm2] area

Cornea: 3.5 [mm] diameter; 9.62e-2 [cm2] area

F. Maximum power

At 1280 nm (previously used in calculations)

- Retina: 45.9 mW
- Cornea: 52.5 mW
- Skin: 96.2 mW

At 1300 nm:

- Retina: 207.9 mW
- Cornea: 35.6 mW
- Skin: 96.2 mW

As a function of wavelength:

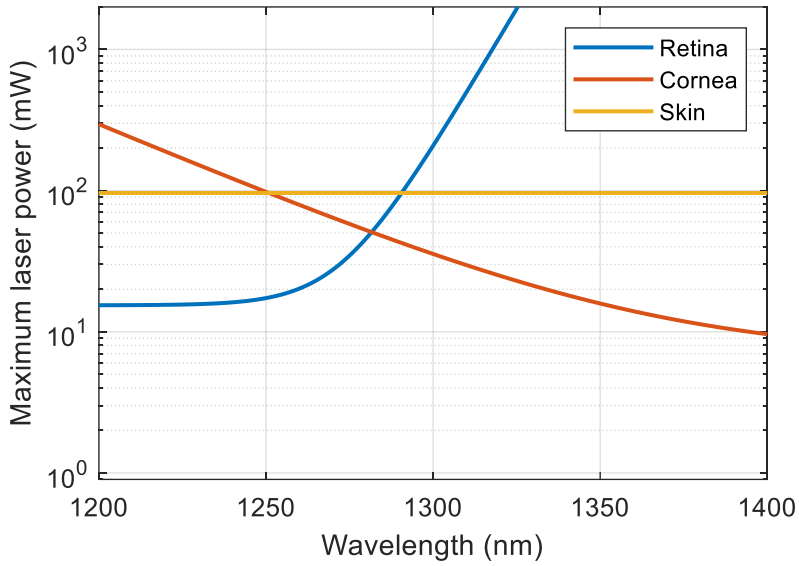

G. Average MPE weighted by the source spectrum:

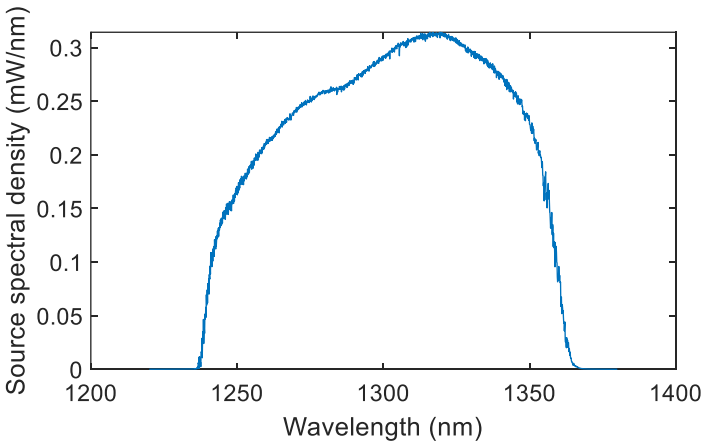

- Retina: 68.6 mW
- Cornea: 30.0 mW
- Skin: 96.2 mW

H. References for broadband calculation:

F. C. Delori, R. H. Webb, and D. H. Sliney, "Maximum permissible exposures for ocular safety (ANSI 2000), with emphasis on ophthalmic devices," J. Opt. Soc. Am. A **24**, 1250 (2007). [section 8]

I. Detailed derivation of broadband calculation:

Starting from Eq.24 in Delori et al (2000), in continuous form:

$$\int \frac{\phi(\lambda)}{MP\Phi(\lambda)} d\lambda < 1$$

Where $\phi(\lambda)$ is the source power spectral density [mW/nm], and $MP\Phi(\lambda)$ is the maximum permissible radiant power [mW].

Define Φ_{tot} the total power of the laser (measured with a power meter):

$$\Phi_{tot} = \int \phi(\lambda)\, d\lambda$$

This equation implies:

$$\phi(\lambda) = \Phi_{tot}\left[\frac{\phi(\lambda)}{\int \phi(\lambda) d\lambda}\right] = \Phi_{tot}\tilde{\phi}(\lambda)$$

The term between square brackets, noted $\tilde{\phi}(\lambda)$, represents a normalized power spectrum, which can be calculated regardless of the units and at any point in the system (such as measured with an OSA). Substituting in the MPE equation:

$$\int \frac{\phi(\lambda)}{MP\Phi(\lambda)} d\lambda = \Phi_{tot} \int \frac{\tilde{\phi}(\lambda)}{MP\Phi(\lambda)} d\lambda < 1$$

If we rearrange the terms, we can express in the form of a maximal total power $\Phi_{\max}$:

$$\Phi_{tot} < \left(\frac{\int \phi(\lambda) \left(MP\Phi(\lambda)\right)^{-1} d\lambda}{\int \phi(\lambda)\, d\lambda}\right)^{-1} = \Phi_{\max}$$

Which is the equation implemented in the Matlab code.

NOTE: this equation implies that the response of the photodetector used to measure the total power is relatively flat around the center wavelength.

XIII. REFERENCES

1. Morishige N, Wahlert AJ, Kenney MC, Brown DJ, Kawamoto K, Chikama T-i, et al. Second-harmonic imaging microscopy of normal human and keratoconus cornea. Investigative ophthalmology & visual science. 2007;48(3):1087-94.
2. Dupps WJ, Wilson SE. Biomechanics and wound healing in the cornea. Experimental eye research. 2006;83(4):709-20.
3. Dawson DG, Randleman JB, Grossniklaus HE, O'Brien TP, Dubovy SR, Schmack I, et al. Corneal ectasia after excimer laser keratorefractive surgery: histopathology, ultrastructure, and pathophysiology. Ophthalmology. 2008;115(12):2181-91. e1.
4. Wollensak G, Spoerl E, Seiler T. Riboflavin/ultraviolet-A–induced collagen crosslinking for the treatment of keratoconus. American journal of ophthalmology. 2003;135(5):620-7.

5. de Sanctis U, Loiacono C, Richiardi L, Turco D, Mutani B, Grignolo FM. Sensitivity and specificity of posterior corneal elevation measured by Pentacam in discriminating keratoconus/subclinical keratoconus. Ophthalmology. 2008;115(9):1534-9.
6. Li X, Rabinowitz YS, Rasheed K, Yang H. Longitudinal study of the normal eyes in unilateral keratoconus patients. Ophthalmology. 2004;111(3):440-6.
7. Pallikaris IG, Kymionis GD, Astyrakakis NI. Corneal ectasia induced by laser in situ keratomileusis. Journal of Cataract & Refractive Surgery. 2001;27(11):1796-802.
8. Binder PS, Lindstrom RL, Stulting RD, Donnenfeld E, Wu H, McDonnell P, et al. Keratoconus and corneal ectasia after LASIK. Journal of refractive surgery. 2005;21(6):749-52.
9. Rabinowitz YS. Ectasia after laser in situ keratomileusis. Current opinion in ophthalmology. 2006;17(5):421-6.
10. Elsheikh A, Wang D, Brown M, Rama P, Campanelli M, Pye D. Assessment of corneal biomechanical properties and their variation with age. Current eye research. 2007;32(1):11-9.
11. Cartwright NEK, Tyrer JR, Marshall J. Age-related differences in the elasticity of the human cornea. Investigative ophthalmology & visual science. 2011;52(7):4324-9.
12. Ruberti JW, Sinha Roy A, Roberts CJ. Corneal biomechanics and biomaterials. Annual review of biomedical engineering. 2011;13:269-95.
13. Luce DA. Determining in vivo biomechanical properties of the cornea with an ocular response analyzer. Journal of Cataract & Refractive Surgery. 2005;31(1):156-62.
14. Kirwan C, O'Malley D, O'Keefe M. Corneal hysteresis and corneal resistance factor in keratoectasia: findings using the Reichert ocular response analyzer. Ophthalmologica. 2008;222(5):334-7.
15. Bak-Nielsen S, Pedersen IB, Ivarsen A, Hjortdal J. Dynamic Scheimpflug-based assessment of keratoconus and the effects of corneal cross-linking. Journal of refractive surgery. 2014;30(6):408-14.
16. Dorronsoro C, Pascual D, Pérez-Merino P, Kling S, Marcos S. Dynamic OCT measurement of corneal deformation by an air puff in normal and cross-linked corneas. Biomedical optics express. 2012;3(3):473-87.
17. Kling S, Bekesi N, Dorronsoro C, Pascual D, Marcos S. Corneal viscoelastic properties from finite-element analysis of in vivo air-puff deformation. PLoS One. 2014;9(8):e104904.
18. Tanter M, Touboul D, Gennisson J-L, Bercoff J, Fink M. High-resolution quantitative imaging of cornea elasticity using supersonic shear imaging. IEEE transactions on medical imaging. 2009;28(12):1881-93.
19. Ford MR, Dupps WJ, Rollins AM, Roy AS, Hu Z. Method for optical coherence elastography of the cornea. Journal of biomedical optics. 2011;16(1):016005--7.
20. Nguyen T-M, Song S, Arnal B, Wong EY, Huang Z, Wang RK, et al. Shear wave pulse compression for dynamic elastography using phase-sensitive optical coherence tomography. Journal of biomedical optics. 2014;19(1):016013-.
21. Kennedy BF, Kennedy KM, Sampson DD. A review of optical coherence elastography: fundamentals, techniques and prospects. IEEE Journal of Selected Topics in Quantum Electronics. 2014;20(2):272-88.
22. Adie SG, Liang X, Kennedy BF, John R, Sampson DD, Boppart SA. Spectroscopic optical coherence elastography. Optics express. 2010;18(25):25519-34.

23. Twa MD, Li J, Vantipalli S, Singh M, Aglyamov S, Emelianov S, et al. Spatial characterization of corneal biomechanical properties with optical coherence elastography after UV cross-linking. Biomedical optics express. 2014;5(5):1419-27.
24. Li C, Guan G, Huang Z, Johnstone M, Wang R. Noncontact all-optical measurement of corneal elasticity. Optics letters. 2012;37(10):1625-7.
25. Scarcelli G, Yun SH. Confocal Brillouin microscopy for three-dimensional mechanical imaging. Nature photonics. 2008;2(1):39-43.
26. Fercher AF, Drexler W, Hitzenberger CK, Lasser T. Optical coherence tomography-principles and applications. Reports on progress in physics. 2003;66(2):239.
27. Chinn S, Swanson E, Fujimoto J. Optical coherence tomography using a frequency-tunable optical source. Optics letters. 1997;22(5):340-2.
28. Yun S-H, Tearney GJ, de Boer JF, Iftimia N, Bouma BE. High-speed optical frequency-domain imaging. Optics express. 2003;11(22):2953-63.
29. Yun S, Tearney G, de Boer J, Shishkov M, Oh W, Bouma B. Catheter-based optical frequency domain imaging at 36 frames per second. Coherence Domain Optical Methods and Optical Coherence Tomography in Biomedicine IX, 5690. 2005;16.
30. Vakoc BJ, Shishko M, Yun SH, Oh W-Y, Suter MJ, Desjardins AE, et al. Comprehensive esophageal microscopy by using optical frequency–domain imaging (with video). Gastrointestinal endoscopy. 2007;65(6):898-905.
31. Huber R, Wojtkowski M, Fujimoto JG, Jiang J, Cable A. Three-dimensional and C-mode OCT imaging with a compact, frequency swept laser source at 1300 nm. Optics Express. 2005;13(26):10523-38.
32. Yasuno Y, Madjarova VD, Makita S, Akiba M, Morosawa A, Chong C, et al. Three-dimensional and high-speed swept-source optical coherence tomography for in vivo investigation of human anterior eye segments. Optics Express. 2005;13(26):10652-64.
33. Zhang J, Chen Z. In vivo blood flow imaging by a swept laser source based Fourier domain optical Doppler tomography. Optics express. 2005;13(19):7449-57.
34. Choma MA, Hsu K, Izatt JA. Swept source optical coherence tomography using an all-fiber 1300-nm ring laser source. Journal of biomedical optics. 2005;10(4):044009--6.
35. Huber R, Wojtkowski M, Taira K, Fujimoto JG, Hsu K. Amplified, frequency swept lasers for frequency domain reflectometry and OCT imaging: design and scaling principles. Optics Express. 2005;13(9):3513-28.
36. Yun S, Tearney G, De Boer J, Bouma B. Motion artifacts in optical coherence tomography with frequency-domain ranging. Optics Express. 2004;12(13):2977-98.
37. Lee EC, de Boer JF, Mujat M, Lim H, Yun SH. In vivo optical frequency domain imaging of human retina and choroid. Optics Express. 2006;14(10):4403-11.
38. Chang EW, Kobler JB, Yun SH. Subnanometer optical coherence tomographic vibrography. Optics letters. 2012;37(17):3678-80.
39. Akca BI, Chang EW, Kling S, Ramier A, Scarcelli G, Marcos S, et al. Observation of sound-induced corneal vibrational modes by optical coherence tomography. Biomedical optics express. 2015;6(9):3313-9.
40. Kling S, Akca IB, Chang EW, Scarcelli G, Bekesi N, Yun S-H, et al. Numerical model of optical coherence tomographic vibrography imaging to estimate corneal biomechanical properties. Journal of The Royal Society Interface. 2014;11(101):20140920.

41. Vaughan J, Randall J. Brillouin scattering, density and elastic properties of the lens and cornea of the eye. Nature. 1980;284(5755):489-91.
42. Scarcelli G, Kim P, Yun SH. In vivo measurement of age-related stiffening in the crystalline lens by Brillouin optical microscopy. Biophysical journal. 2011;101(6):1539-45.
43. Elsheikh A, Wang D, Pye D. Determination of the modulus of elasticity of the human cornea. Journal of refractive surgery. 2007;23(8):808-18.
44. Wah T. Vibration of circular plates. the Journal of the Acoustical Society of America. 1962;34(3):275-81.
45. Younesian D, Aleghafourian MH, Esmailzadeh E. Vibration analysis of circular annular plates subjected to peripheral rotating transverse loads. Journal of Vibration and Control. 2015;21(7):1443-55.